



Novel Xylazine voltammetric sensors based on zinc oxide nanostructure

Hassan A.M. Hendawy¹  and Elmorsy Khaled^{2,*} 

¹National Organization for Drug Control and Research (NODCAR), P.O. Box 29, Cairo, Egypt

²Applied Organic Chemistry Department, National Research Centre, El Bohouth St., Dokki, 12622 Giza, Egypt



CrossMark

Abstract

Xylazine (XYL) is veterinary drug administrated for sedative and analgesic purposes. With severe side effects, XYL is not approved for the human use. Recently, XYL has been categorized as a drug of abuse, and has been associated with drug-facilitated sexual assaults. Therefore, the present study described the electrochemical behavior of XYL at novel carbon paste working electrodes integrated with different metallic oxides nanoparticles. Among them, carbon paste matrices fortified with zinc oxide nanoparticles (ZnONPs) showed a noticeable electrocatalytic activity towards the oxidation of XYL with an anodic irreversible oxidation peak at 0.885 V in Britton-Robinson (pH 7.0). Oxidation of XYL molecule at the electrode surface followed diffusion-reaction mechanism through the participation of two-electrons and two protons as confirmed by the molecular orbital calculations and electroanalytical parameters studies. A simple and accurate quantification protocol using square wave voltammetry offered enhanced sensitivity towards XYL within a wide concentration range from 29 to 806 ng mL⁻¹ XYL, with limit of detection 5.44 ng mL⁻¹. The fabricated sensors showed high measurement reproducibility with a prolonged. The ZnONPs/CPEs were introduced for monitoring of XYL residues in veterinary matrices with high accuracy and precision. Moreover, to forensic scenario, a standard addition technique on plasma and urine samples revealed acceptable recovery values, demonstrating the potentiality to forensic and clinical analysis of xylazine intoxication.

Keywords: Xylazine; Zinc oxide nanoparticle; carbon paste electrodes; Square wave voltammetry; Veterinary formulations; Forensic scenario.

1. Introduction

Xylazine, (XYL, N-(2,6-dimethylphenyl)5,6-dihydro-4H-1,3-thiazin-2-amine), represents an α -2-agonist sedative drug first developed by Farbenfabriken Bayer as a medicinal drug for the treatment of hypertension [1, 2]. XYL was approved by the Food and Drug Administration (FDA) as a central nerve system depressant veterinary drug primarily used to induce a state of sedation with a shorter interval of analgesic, preanesthetic prior to general or local anesthesia, and as an immobilisation agent for large wild animals [3, 4]. XYL stimulates the central α 2-receptors, and thus inhibits the release of peripheral norepinephrine, causing bradycardia, hypotension, and reduced cardiac output [5]. Although XYL is used legitimately as tranquilizer in veterinary science, there are still reservations regarding its usage in specific industries, particularly the drug industry, animal production industry, and animal doping

industry. Currently, XYL is categorized as a controlled substance in many countries [6], and is scheduled as a poison. However, due to its central nervous system depressant effects, the FDA banned its use by humans [7], as it could cause hazardous side effects, and even death. Several reports associated with XYL misuse by humans were reviewed [8, 9]. Moreover, the unconventional use of XYL has also been reported in food-producing animals as well as sport animals [10, 11]. Other its deleterious side effects such as bradycardia, hypotension, and possibly death [12, 13]. According to the FDA, the use of XYL in “food-producing animals” is specifically not allowable, but in some countries, XYL can legally be used in food producing animals [9].

Drug-facilitated crime (DFC, crimes committed whenever victims of the crime) are placed under the influence of drugs is a serious issue worldwide [14]. To increase its effectiveness when used illicitly, XYL is usually co-administered with other drugs such as heroin, cocaine, or ketamine. XYL facilitates sexual assaults and robbery as the victims

*Corresponding author e-mail: elmorsykhaled@yahoo.com

Receive Date: 08 August 2023, Revise Date: 24 August 2023, Accept Date: 04 September 2023

DOI: 10.21608/EJCHEM.2023.228115.8398

©2023 National Information and Documentation Center (NIDOC)

cannot remember events while they were under the influence of XYL [15]. The victim had previously unknowingly consumed food that was spiked with drugs; in other words, drugs originally designed for medicinal or veterinary use have been illegally used to incapacitate victims by exploiting the pharmacological effects of such drugs [16, 17]. Common examples for DFC include benzodiazepine, ketamine, gamma hydroxybutyrate and more recently XYL [18, 19]. In view of its potential abuse in DFC, the searching of forensic evidence and successful detection of illicit drug contained in drug-spiked beverages and foods is crucial for obtaining justice for victims.

XYL has gained popularity as a recreational drug worldwide [9, 20, 21] and is largely used as an adulterant of drugs of abuse such as cocaine, heroin, and speedball [9, 22]. Therefore, a precise and accurate analytical approach was required for monitoring XYL residues in biological fluids. Previous studies have suggested various instrumental chromatographic techniques including gas chromatography (GC) [23-25], liquid chromatography [24, 26], and thin layer chromatography [12]. However, chromatographic techniques require expert personnel to operate the sophisticated high-cost instruments and performing a tedious sample pretreatment process.

Electroanalytical approaches with the aid of modified electrochemical sensors were encouraged for detection of pharmaceutical residues applying simple instrumentation requirements and sample pretreatment steps [27-30]. Electrochemical techniques ranked third, behind photometry and chromatography for monitoring the drugs contaminants in food and environmental samples. To the best of our knowledge, few electroanalytical approaches were reported for voltammetric assaying of XYL based on the conventional glassy carbon electrodes [31, 32], carbon paste matrix integrated with multiwalled carbon nanotube (MWCNTs/CPE) [33], graphene nanoplatelets-modified screen-printed carbon electrode (GNPs/SPCE) [34], electrochemical paper-based analytical device (ePAD) coated with graphene printing ink [35], or laser-scribed graphene (LSG) device [36].

Studies were executed to fortify the matrix of voltammetric sensor with various metallic nanostructures to improve the sensor performance [37-39]. Nanostructure based sensors improve the future of the procedure with a nonedible increase in the selectivity and sensitivity of the method. Awing to the electrocatalytic activity of the electrode modifier, the redox potential of the target analyte was shifted towards the negative direction, and the kinetics of electron transfer process at the electrode surface was accelerated. This study characterized the electrochemical futures of a novel carbon paste sensor

integrated with zinc oxide nanoparticles (ZnONPs/CPE) for sensitive square wave voltammetric determination of xylazine in veterinary formulations and biological samples. The impact of various electroanalytical parameters, the nature and content of the electrode modifier, pH of the supporting electrolyte, sweep rate, and tentative electrode reaction mechanism were evaluated.

2. Experimental

2.1. Chemicals

Analytical grade reagents and ultrapure water (Milli-Q system, Millipore, with electric resistivity $\sim 18.3 \text{ M}\Omega \text{ cm}$) were used for the preparation of supporting electrolyte and stock solutions. The xylazine hydrochloride standard sample ($\text{C}_{12}\text{H}_{16}\text{N}_2\text{S}$, $256.80 \text{ g mol}^{-1}$, with purity $99.25 \pm 1.05\%$, was kindly provided by Laboratory Standard, Egyptian Drug Authority). Stock XYL solution was prepared with bidistilled water and stored in refrigerator at $4 \text{ }^\circ\text{C}$. Graphite powder and paraffin oil (Sigma-Aldrich), were applied for construction of the bare carbon paste matrix. Metal oxides nanostructures including; zinc oxide nanopowders, iron oxide nanopowder ($<50 \text{ nm}$), and copper oxide nanopowder, were purchased from Sigma-Aldrich. Britton-Robinson (BR) stock solution ($4 \times 10^{-2} \text{ mol L}^{-1}$) was prepared by dissolving 2.47 g boric acid in a mixture of 2.7 mL phosphoric acid, and 2.3 mL glacial acetic acid, and diluted to 1 liter with deionized water. The desired pH value was adjusted with sodium hydroxide solution.

2.2. Zinc oxide integrated working electrodes and measuring system

797 VA Metrohm station (Metrohm, Switzerland) accompanied with platinum wire, silver/silver chloride, and the homemade carbon paste electrodes as auxiliary, reference, and working electrodes, respectively was applied for voltammetric measurements. Carbon paste working electrodes were fortified with zinc oxide nanostructure through mixing 10 mg of ZnONPs, 190 mg graphite powder with 80 μL of paraffin oil as a proper pasting liquid. After careful blending of the paste components for 15 min in an agate mortar, and the resulting homogeneous paste was packed into the Teflon electrode body with 3 mm radii [40]. Prior to voltammetric measurements, the electrode surface was regenerated through polishing with a wet filter paper.

2.3. Determination of the electroactive surface area

To calculate the electroactive surface area of the fabricated sensors, cyclic voltammograms were recorded in $5 \times 10^{-3} \text{ mol L}^{-1} \text{ K}_4[\text{Fe}(\text{CN})_6]$ solution at different scan rate values. The peak currents of the recorded CVs were linearly correlated with the scan rate value indicating a diffusion-controlled process at the electrode surface and the electrode surface area

was estimated according to Randles-Sevcik equation [41, 42].

2.4. Measuring procedures

At the optimized electrode matrix composition, ascending increments of the standard XYL solution were added to the thermostated measuring cell at 25 ± 1.0 °C containing 15 mL BR buffer solution at pH 7. Square wave voltammograms were recorded at the optimal measuring parameters; voltage step 6 mV, amplitude 20 mV, frequency 50 Hz, and scan rate 0.3 V. The recorded peak heights (based on the baseline subtraction) were plotted against the corresponding XYL concentration. All experiments were performed at room temperature under atmospheric conditions.

2.5. Sample analysis

PROXYLAZ® (2.0 % Injectable solution, Prodivet pharmaceutical Company, Belgian, each mL contains 20 mg of XYL) was purchased from local veterinary stores. After appropriate dilution, different aliquots of the commercial samples were transferred to the measuring cell and assayed according to the recommended voltammetric approach in comparison with the chromatographic ones.

Standard plasma samples (VACSERA, Dokki, Giza) were fortified with known aliquots of the XYL stock standard solution, vortexed with acetonitrile (2:1 ratio), and centrifuged at 10000 rpm for 10 min at 4°C to remove the residual protein. Urine samples were laced with aliquots of the standard XYL solution, treated with methanol to remove protein. The XYL contents in both clear supernatants were analyzed voltammetrically compared with the official method.

2.6. Molecular orbital calculations

Molecular orbital calculations applying Hukel, MM94, and MOPAC models were performed to explain the tentative XYL oxidation mechanism at the ZnONPs/CPEs. Such estimations were performed with Gaussian chem office 2017 suite programs [43, 44].

3. Results and discussion

3.1. Electrochemical oxidation of XYL at ZnONPs/CPE

At the bare carbon paste surface, xylazine was irreversibly oxidized with a single anodic oxidation broad peak at 0.952 V (**Figure 1a**). The broad peak and limited current density may be attributed to the sloth electron transfer at the electrode surface. Upon integration of the electrode matrix with different metallic nanostructures, the electrode performance was enhanced based on their electrocatalytic activity, improvement of the electroactive surface area and facilitation of the electron transfer process at the electrode surface. Both copper oxide and iron oxide nanoparticles exhibited relatively lower peak currents compared with ZnONPs due to the difference in their overall redox potentials and band gaps values.

Next, carbon paste matrices fortified with different amounts of ZnONPs were tested for voltammetric determination of XYL (**Figure 1b**). Gradual improvement of the peak current was reported via incorporation of ZnONPs in the electrode matrix with a maximum peak height at 5.0% modifier (about 5 folds amplification compared with the plain carbon paste electrode). Higher content of the modifier diminished the electrode performance based on changing of paste homogeneity and the requirement for the additional amounts of the pasting liquid.

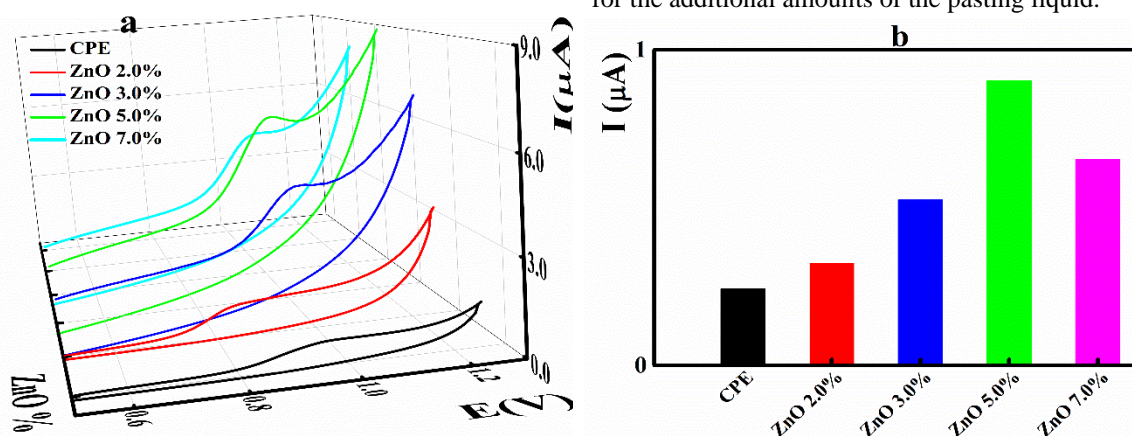


Figure 1: a) Cyclic voltammograms recorded for $4.0 \mu\text{g mL}^{-1}$ XYL at ZnONPs/CPEs with different ZnONPs ratios; and b) peak height against ZnONPs ratio. Scan rate 60 mVs^{-1} at pH 7.

The electroactive surface area of the fabricated ZnONPs/CPEs were evaluated through recording the CVs at different sweep rate in FCN

solution as the standard redox probe. Shifting of the peak potential with improved peak current provide compelling evidence for the electrocatalytic function

of zinc oxide nanostructure. According to Randles-Sevcik equation [41, 42], the resulted electroactive areas were found to be 0.027, 0.039, 0.070, 0.105 and 0.115 cm² for the bare electrode compared with those integrated with different ZnO ratios.

3.2. Electrochemical behavior of XYL at different pH

Xylazine showed pKa value of 6.94; therefore, its electrochemical behavior is expected to be pH controlled. Square wave voltammograms for XYL were recorded in BR supporting electrolyte having different pH values ranging from 2 to 10 (**Figure 2a**). At lower pH values (2, 3), broad and low current values peaks were recorded. At evaluated pH values, gradual improvement of the peak current was

achieved with a maximum current value at pH 7 (**Figure 2a, b**). It is noteworthy to mention that the achieved results agreed with the previously reported voltammetric XYL methods [31, 33]. The selected pH value is typically equal the pKa of XYL.

As illustrated in figure 2a, the oxidation peak potentials were shifted to more negative values at evaluated pH values postulating the participation of the proton in the electrode reaction [41, 42]. The recorded peak potentials were linearly correlated to the pH value of the supporting electrolyte with a typically Nernstian slope value indicating the participation of equal numbers of electrons and protons in the XYL oxidation [**Fig. 2b**, $E_{ox} (V) = 1.298 - 0.057 [pH]$, $r = 0.9946$].

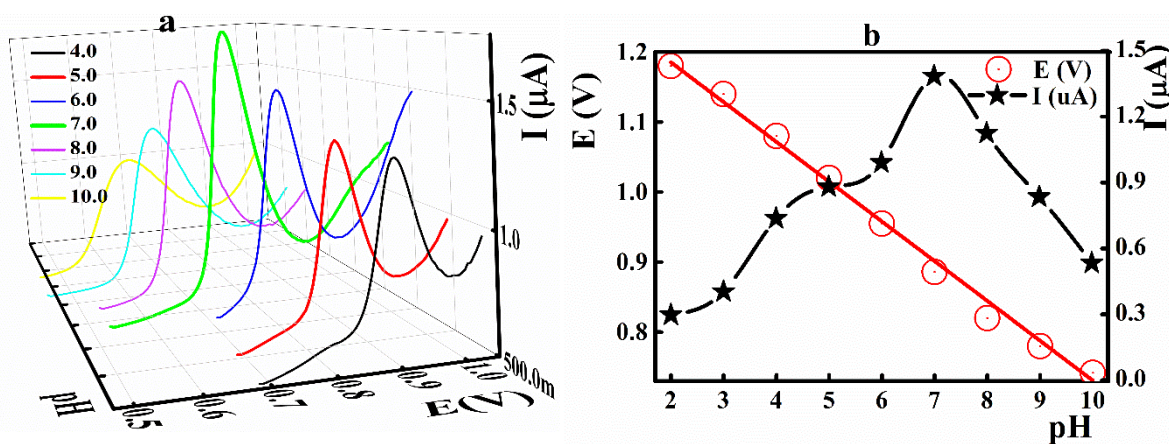


Figure 2: a) Square wave voltammograms recorded for 4.0 µg mL⁻¹ XYL at ZnONPs/CPE applying different pH values; b) relation between peak potentials and peak current versus the pH value.

3.3. Electrochemical behavior at different sweep rates

Performing the cyclic voltametric measurements at different scan rates represents a useful tool for discussion of the electrode reaction, such as reversibility of the electrochemical oxidation process, mechanism of the surface reaction process whether diffusion or adsorption-controlled, kinetic parameters, and the number of electrons transferred in the oxidation process [42]. Therefore, cyclic voltammograms for XYL were recorded at different sweep rate values (**Figure 3a**). Oxidation of XYL molecules at ZnONPs/CPEs resulted in an irreversible single anodic oxidation peak with potential values shifted towards the anodic direction and evaluated peak current values at higher sweep rates indicating the irreversibility of the electrode reaction. Within the whole tested scan rates, a

linear plot was illustrated between the peak current and the square root value of the scan rate (**Figure 3b**) suggesting the irreversibility of the electrode reaction. Moreover, plotting the logarithmic value of the peak current against the logarithmic value of the scan rate (**Figure 3c**) showed a linear relationship [$\log(I_{\mu A}) = 0.5203 \log v (Vs^{-1}) + 0.3224$; $r=0.9996$] with slope value near to the theoretical value of the diffusion-controlled reaction [45, 46]. The peak potential values were shifted to the positive direction at higher scan rate following a linear equation [**Figure 3d**; $E_{ox(V)} = 0.9956 + 0.0989 [\log(v/Vs^{-1})]$, $r=0.9988$] indicating the transfer of 1.673 (2 electrons) in the electrooxidation process [47].

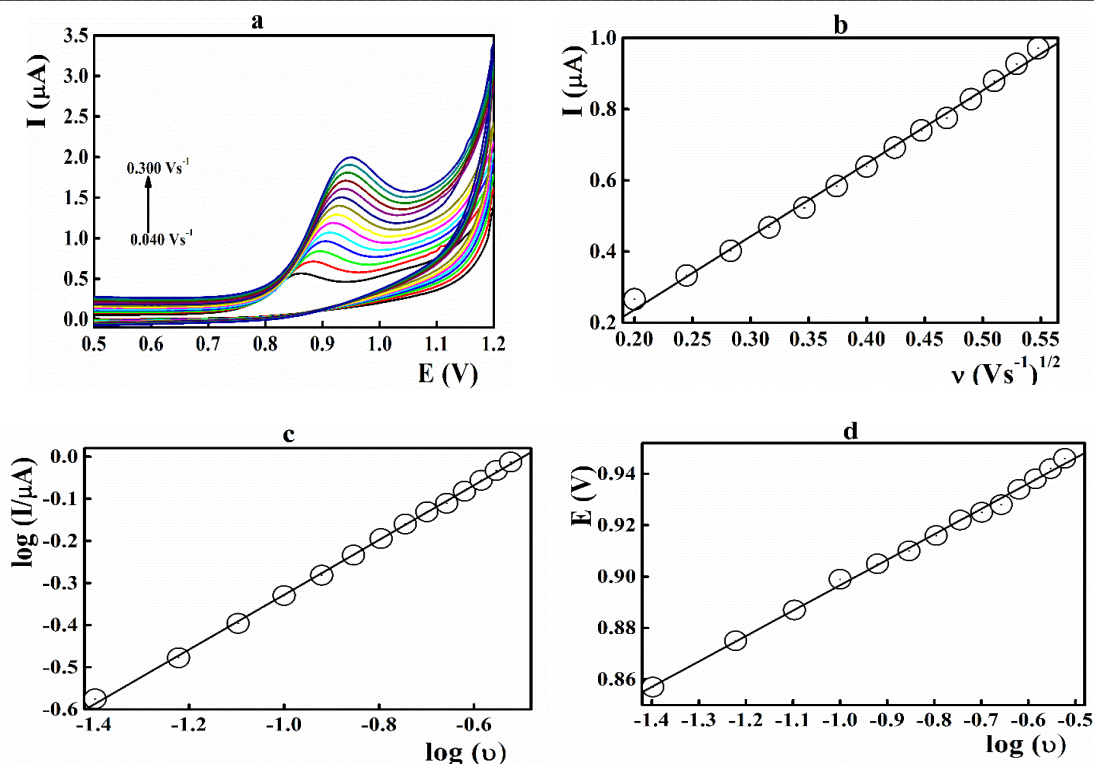
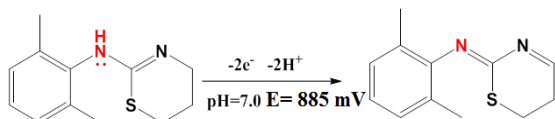


Figure 3: a) The recorded CVs for $3.0 \mu\text{g mL}^{-1}$ XYL at different scan rate values, b) values of the peak current at different scan rates against the square root of the scan rate, c) the estimated logarithmic value of the peak current at different scan rates against logarithmic value of the corresponding scan rate, and d) the recorded peak potential against logarithmic value of the scan rate.

Based on the molecular orbital calculations on xylazine molecule (**Table 1**), the most probable oxidation mechanism of XYL takes place through oxidation of the nitrogen atom (N7) in the amino group within the xylazine moiety which recorded higher electrically negative charge owing to the presence of lone pair of electrons; therefore, it is the highest candidate to loss electrons compared with the rest of atoms in the XYL molecule.

Other nitrogen atom presents in the thiazin ring (N3) was involved in resonance process which diminish the effect of the free pair of electrons at N3. In the projected method, the electrooxidation of XYL was assumed to include two electrons and two protons (see sec 3.2. and 3.3.), and the tentative mechanism was illustrated in **Scheme 1**.



Scheme 1: Electrochemical oxidation of xylazine at the ZnONPs/CPE at pH 7.0

3.4. Linearity range and validation of the method

At the optimized sensor matrix composition and electroanalytical parameters, the performance characteristics of the ZnONPs/CPEs against xylazine were evaluated. Different ascending aliquots of the stock XYL solution were spiked to the measuring cell at pH 7, and the registered square wave voltammograms (SWVs) were plotted versus the XYL concentration (**Figure 4 & Table 2**). The illustrated calibration graphs were rectilinear ($r=0.9999$) within a wide XYL concentration ranged from 29 to 806 ng mL^{-1} . The high correlation coefficient with low standard deviation values confirmed the applicability of the proposed analysis protocol for XYL quantification within the cited concentration range. Based on the linearity parameters, the limit of detection (LOD) and limit of quantification (LOQ) were estimated to be 5.44 and 16.94 ng mL^{-1} , respectively applying the relations $\text{LOQ}=10*(\text{SD}/S)$ and $\text{LOD}=3.3*(\text{SD}/S)$, where SD is the standard deviation of the intercept and S is the slope of the calibration curve [48].

Table 1: Computed molecular orbital calculations of xylazine molecules

Atom	Atom Type (MM2)	Charge (MM2)	Charge (Huckel)	Atom (MMFF94)	Type	Charge (MMFF94)	Mulliken Charges (Mopac Interface)
S(1)	S Thioether	0	0.0649768	THIOL, SULFIDE, DISULFIDE	SULFUR	OR	-0.275195
C(2)	C Alkane	0	0.144166	ALKYL CARBON, SP3		0.8451	0.279842
N(3)	N Imine	0	-0.265116	IMINE NITROGEN		-0.696	-0.534227
C(4)	C Alkene	0	0.140023	SP2 CARBON IN C=N		0.329	0.137146
C(5)	C Alkane	0	-0.107548	ALKYL CARBON, SP3		0.061	-0.448288
C(6)	C Alkane	0	-0.0543832	ALKYL CARBON, SP3		0.23	-0.367558
N(7)	N Enamine	0	0.195276	ENAMINE OR ANILINE NITROGEN, DELOC. LP		-0.8691	-0.677794
C(8)	C Alkene	0	0.115278	AROMATIC CARBON, E. G. IN BENZENE, PYRIDIN		0.1	0.129935
C(9)	C Alkene	0	-0.0700462	AROMATIC CARBON, E. G. IN BENZENE, PYRIDIN		-0.1435	-0.011895
C(10)	C Alkene	0	-0.0706923	AROMATIC CARBON, E. G. IN BENZENE, PYRIDIN		-0.15	-0.215864
C(11)	C Alkene	0	-0.204904	AROMATIC CARBON, E. G. IN BENZENE, PYRIDIN		-0.15	-0.198068
C(12)	C Alkene	0	-0.0622209	AROMATIC CARBON, E. G. IN BENZENE, PYRIDIN		-0.15	-0.226668
C(13)	C Alkene	0	-0.103732	AROMATIC CARBON, E. G. IN BENZENE, PYRIDIN		-0.1435	0.020656
C(14)	C Alkane	0	-0.152234	ALKYL CARBON, SP3		0.1435	-0.58394
C(15)	C Alkane	0	-0.142088	ALKYL CARBON, SP3		0.1435	-0.592115

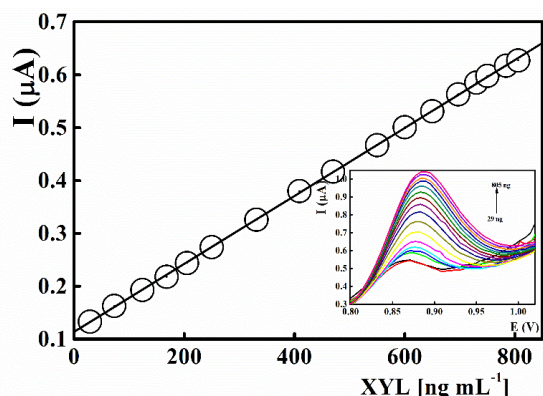


Figure 4: Square wave voltammetric determination of xylazine at ZnONPs/CPE; the working pH value was 7.

Compared with voltammetric approach based on GCE and rG/SPE [32, 35], the presented method showed improved performance (more than twenty-fold sensitivity), with the ease of fabrication and regeneration of the electrode surface (Table 3). Moreover, ZnONPs based carbon paste sensors, showed oxidation peak for XYL molecule at more negative potential compared with the MWCNTs/CPE [34] with better performance and prolonged operational lifetime which can be explained on the bases of the oxidative catalytic activity of the electrode

modifier (ZnONPs) and facilitation of XYL oxidation at the electrode surface compared with MWCNTs. Meanwhile the rG/SPE based sensors [35] can operate only for few runs; the presented carbon paste electrode modified in bulk with ZnONPs can be utilized for more than 2 months without diminishing its performance. The ease of the carbon paste fabrication and its availability in research laboratories represents promising advantages compared with the disposable XYL sensors [36, 37].

In order to evaluate the repeatability of the peak current, seven successive square voltammograms were recorded for 150 ng mL⁻¹ XYL solution at the same electrode surface. The ZnONPs/CPEs showed high repeatability of measurement, expressed as percentage relative standard deviation, the estimated RDS value was 1.27 %. Integration of the electrode matrix with metal oxide nanostructure improved the measuring repeatability and minimizes accumulation of the XYL at the electrode surface based on its antifouling function and improvement of the electroactive surface area. Moreover, one of most promising advantages of carbon paste sensors is the ease of electrode regeneration process through simple polishing of the paste surface with a wet filter paper compared with tedious polishing of GCE with alumina powder.

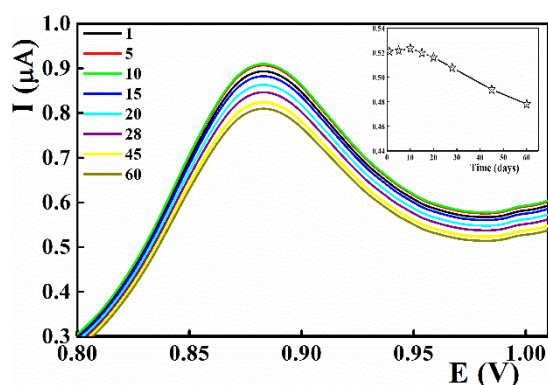
Table 2: Squar wave voltammetric determination of xylazine at ZnONPs/CPE

Parameters	Value
Optimal pH value	7.0
Oxidation potential (V)	0.885
Linearity rang (ng mL ⁻¹)	29-806
Intercept (μA cm ⁻²)	0.1138
SD of intercept (μA cm ⁻²)	0.0010
Slope (μA mL ⁻¹ /ng)	0.00064
SD of slope (μA mL ⁻¹ /ng)	2.0347×10 ⁻⁶
Multiple R	0.9999
Standard Error	0.0245
RSD	0.5453
LOD (ng mL ⁻¹)	5.44
LOQ (ng mL ⁻¹)	16.49
Operational lifetime (month)	2
Peak current reproducibility (RSD %) ^a	0.842
Peak current repeatability of the (RSD %) ^a	1.33
Reproducibility of the peak potential (RSD %) ^a	1.5
Repeatability of the peak potential (RSD %) ^a	1.08

Table 3: Performance characteristics of different Xylazine sensors

Sensor	Voltammetric technique	Linear range (×10 ⁻⁶ mol L ⁻¹)	LOD value (×10 ⁻⁶ mol L ⁻¹)	Ref.
GCE	DPV	0.5 to 256	0.12	31
MWCNTs/CPE	DPV	0.05 to 1.5	0.005	33
GNPs/SPCE	DPV	1.8 to 27.2	1.823	34
ePAD	DPV	0.2 to 100	0.272	35
LSG	SWV	5.0 to 200	0.139	36
ZnONPs/CPE	SWV	0.06 to 1.08	0.002	Present

The operational life time of the fabricated ZnONPs/CPEs were evaluated during a prolonged measuring period via recording of the SWVs for 150 ng mL⁻¹ XYL under the same experimental conditions. During the first 28 days, the peak heights of the SWVs remains constant with 96.52% recovery of the original peak height which was then decreased to reach about 88.8% after 60 days (**Figure 5**).

**Figure 5:** Square wave voltammograms recorded for 150 ng mL⁻¹ XYL at ZnONPs/CPEs after different storage intervals

3.5. Sensor specificity and interference studies

For a newly developed analytical approach, the impact of the interfering species on the analyte signal is one of the major challenges. To describe a new developed method as selective one, the recorded relative error should be ±10% [49]. Therefore, the selectivity of the introduced ZnONPs integrated carbon paste sensor was evaluated against XYL in the coexistence of different additives that usually present in the veterinary medicine, and biological fluids in addition to some other cationic species. SWVs were recorded for a known XYL concentration in measuring solutions containing uric acid (UA) and ascorbic acid (AA) and other metal cations such as Fe³⁺, Zn²⁺, Cu²⁺, Ba²⁺ and Pb²⁺. The average recovery for XYL was calculated as a percentage between the XYL peak current in the absence and presence of the interferent species. Sufficiently good recoveries (about 90.9%) were achieved in the presence of different interferants. Moreover, at the specified working pH value (7.0), both AA and UA exhibited oxidation peaks at 0.250 and 0.050 V, respectively without a noticeable interference on the XYL peak at 0.885 V.

Table 4: Voltammetric determination of xylazine in veterinary and biological samples

Sample	Taken (ng mL ⁻¹)	Found (ng mL ⁻¹)	Bias%	Recovery (%)	HPLC
PROXYLAZ	100	100.5	-0.50	100.50	100.01
	250	248	0.80	99.20	101.08
	400	405	-1.25	101.25	99.93
	650	655	-0.77	100.77	100.11
Mean				100.43	100.28
Variance				0.77	0.29
Observations				4	4
df				3	3
t- test	0.29				
F	2.667296				
t Critical two-tail	2.45				
F Critical one-tail	9.28				
Sample	Added (ng mL ⁻¹)	Found (ng mL ⁻¹)	Bias%	Recovery (%)	HPLC
Plasma	150	152	-1.33	101.33	100.07
	250	251	-0.40	100.40	101.10
	500	506	-1.20	101.20	99.94
	700	695	0.71	99.29	100.12
Mean				100.43	100.28
Variance				0.77	0.29
Observations				4	4
df				3	3
t- test	0.46				
F	3.108664				
t Critical two-tail	2.45				
F Critical one-tail	9.28				
Sample	Added (ng mL ⁻¹)	Found (ng mL ⁻¹)	Bias%	Recovery (%)	HPLC
Urine	80	82	-2.50	102.50	100.07
	150	147	2.00	98.00	98.52
	350	355	-1.43	101.43	100.20
	600	607	-1.17	101.17	102.60
Mean				100.77	100.35
Variance				3.75	2.84
Observations				4	4
df				3	3
t- test	0.33				
F	1.32242				
t Critical two-tail	2.45				
F Critical one-tail	9.28				

*Mean average of three determinations.

3.6. Analysis of xylazine sample

The achieved enhanced specificity and sensitivity of the proposed ZnONPs/CPE against xylazine encourage the application of the introduced sensor for voltammetric detection of drug residues in its veterinary formulation and biological fluids. The tested samples were fortified with known XYL concentration and the residues were estimated voltammetrically and according to the official method. Acceptable recoveries with low relative standard deviation demonstrate the applicability of the presented sensors (Table 4).

4. Conclusion

The present research demonstrates the construction and electrochemical performance of a novel xylazine carbon paste voltammetric sensor integrated zinc oxide nanoparticles. Fortification of the paste matrix with ZnONPs improved the sensor performance within XYL concentration ranged from 29 to 806 ng mL⁻¹ with LOD value of 5.44 ng mL⁻¹ based on its electrocatalytic activity towards the oxidation of xylazine molecule at the electrode surface. The oxidation mechanism of XYL molecule was discussed in details based on the involvement of two electrons/protons and sustained with molecular orbital calculations. The presented sensors showed improved performance compared with the reported XYL sensors with the ease of construction and regeneration, and prolonged operational life time. The influence of interferents and the utilization of the proposed sensors for monitoring of XYL in its veterinary formulation and biological fluids were also presented.

5. Acknowledgments

The authors express their great gratitude to the project fund received from the National Research Centre (NRC, Cairo, Egypt) for the internal grant (No. 13020205).

6. References:

1. C. Dart. Advantages and disadvantages of using alpha-2 agonists in veterinary practice. *Aust. Vet. J.* **77**(11):720–722 (1999).
2. S.A. Greene, and J.C. Thurmon. Xylazine – a review of its pharmacology and use in veterinary medicine. *J. Vet. Pharmacol. Ther.* **11**(4):295–313 (1988).
3. A.G. Gallanosa, D.A. Spyker, J.R. Shipe, and D.L. Morris. Human xylazine overdose: A comparative review with clonidine, phenothiazines, and tricyclic antidepressants. *Clin. Toxicol.* **18**(6):663–78 (1981).
4. D.C. Plumb. *Veterinary drug handbook sixth edition*. PharmaVet Inc 2008, S. Sontakke, G. Umapathy, D. Kumar, and D.N. Sigh. A manual chemical immobilization of wild animals (2017).

5. K.A. Moore, M.G. Ripple, S. Sakinedzad, B. Levine, and D.R. Fowler. Tissue distribution of xylazine in a suicide by hanging. *J. Anal. Toxicol.* **27**(2):110–112 (2003).
6. Xylazine enlisted as controlled medicine in Thailand. *Asean Now* (2013).
7. A. Bayramoglu, M. Saritemur, A. Kocak, M. Omeroglu, and I. Akbas. Xylazine intoxication, a case report. *Med. Reports Case Stud.* **01**(02):1–2 (2016).
8. J.J. Fyffe. Effects of xylazine on humans: A review. *Aust. Vet. J.* **71**(9):294–295 (1994).
9. K. Ruiz Colón, C. Chavez-Arias, J.F. Díaz-Alcalá, and A.M. Martínez. Xylazine intoxication in humans and its importance as an emerging adulterant in abused drugs: A comprehensive review of the literature. *Forensic Science International*, **240**: 1-8 (2014).
10. L. Laitem, I. Bello, and P. Gaspar. Gas chromatography determination of tranquiliser residues in body fluids and in the meat of slaughtered animals. *J. Chromatogr. A* **156**(2):327–329 (1978).
11. Racing Medication and Testing Consortium 2015 report on prohibited substances –2015. <http://rmtcnet.com/wp-content/uploads/IFHA-Prohibited-Substances-2015>
12. U. Hoffmann, C.M. Meister, K. Golle, and M. Zschiesche. Severe intoxication with the veterinary tranquilizer xylazine in humans. *J. Anal. Toxicol.* **25**(4): 245-249 (2001).
13. X. Zheng, X. Mi, S. Li, and G. Chen. Determination of xylazine and 2,6-xylidine in animal tissues by liquid chromatography-tandem mass spectrometry. *Journal of Food Science*, **78**(6): T955-T959 (2013).
14. G. Pépin. The history of drug-facilitated crimes in France. Toxicological aspects of drug facilitated crimes. Academic Press, New York: pp. 1-8 (2014).
15. H. Andresen-Streichert, S. Iwersen-Bergmann, A. Mueller, and S. Anders. Attempted drug-facilitated sexual assault-xylazine intoxication in a child. *J. Forensic Sci.* **62**:270-273 (2017).
16. F. Gharedaghi, H. Hassanian-Moghaddam, M. Akhgari, N. Zamani, and F. Taghadosinejad. Drug-facilitated crime caused by drinks or foods. *Egy. J. Forensic Sci. B* (1): 4-10 (2018).
17. M. Tiemensma, and B. Davies. Investigating drug-facilitated sexual assault at a dedicated forensic centre in Cape Town, South Africa. *Forensic Sci. Int.* **288**: 115-122 (2018).
18. J. Krongvorakul, S. Auparakkitanon, S. Trakulsrichai, P. Sanguanwit, J. Sueajai, N. Noumjad, and W. Wananuku. Use of xylazine in drug-facilitated crimes. *J. Forensic Sci.* **63**(4): 1325-1330 (2018).
19. H. Andresen-Streichert, S. Iwersen-Bergmann, A. Mueller, and S. Anders. Attempted drug facilitated sexual assault—xylazine intoxication in a child. *J. Forensic Sci.* **62**(1): 270-273 (2017).
20. G.M.J. Meyer, and H.H. Maurer, Qualitative metabolism assessment and toxicological detection of

- xylazine, a veterinary tranquilizer and drug of abuse, in rat and human urine using GC–MS, LC–MS n , and LC–HR-MS n. *Anal. Bioanal. Chem.* **405**: 9779–9789 (2013).
21. L. Silva-Torres, C. Veléz, L. Álvarez, and B. Zayas. Xylazine as a Drug of Abuse and Its Effects on the Generation of Reactive Species and DNA Damage on Human Umbilical Vein Endothelial Cells, *J. Toxicol.* **2014**: 1–8 (2014).
22. L.A. Silva-Torres, C. Vélez, J. Lyvia Alvarez, J.G. Ortiz, and B. Zayas, Toxic effects of xylazine on endothelial cells in combination with cocaine and 6-monoacetylmorphine, *Toxicol. Vitro.* **28**:1312–1319 (2014).
23. M. Barroso, E. Gallardo, C. Margalho, N. Devesa, J. Pimentel, and D.N. Vieira. Solid phase extraction and gas chromatographic-mass spectrometric determination of the veterinary drug xylazine in human blood. *J. Anal. Toxicol.* **31**(3): 165-169 (2007).
24. G.M.J. Meyer, M.R. Meyer, B. Mischo, O. Schofer, H.H. Maurer. Case report of accidental poisoning with the tranquilizer xylazine and the anesthetic ketamine confirmed by qualitative and quantitative toxicological analysis using GC-MS and LC-MS. *Drug Testing Anal.* **5**(9-10): 785-789 (2013).
25. N.S.M. Sadiq, W.K. Teoh, K. Saisahas, A. Phonchai, V. Kunalan, N.Z.M. Muslim, W. Limbut, K.H. Chang, and A.F.L. Abdullah, DETERMINATION OF RESIDUAL XYLAZINE BY GAS CHROMATOGRAPHY IN DRUG-SPIKED BEVERAGES FOR FORENSIC INVESTIGATION. *Malaysian J. Anal. Sci.* **26**(4): 774-787 (2022).
26. J. Krongvorakul, S. Auparakkitanon, S. Trakulsrichai, P. Sanguanwit, J. Sueajai, N. Noumjad, and W. Wananukul. Use of xylazine in drug-facilitated crimes. *J. Forensic Sci.* **63**(4): 1325-1330 (2018).
27. M.R. Siddiqui. Z.A. AlOthman, and N. Rahman. Analytical techniques in pharmaceutical analysis: A review. *Arab. J. Chem.* **10**; S1409-S1421 (2017).
28. S.A. Ozkan, Electroanalytical methods in pharmaceutical analysis and their validation. HNB publishing (2012).
29. S.A. Ozkan, J.M. Kauffmann, and P. Zuman. Electroanalysis in biomedical and pharmaceutical sciences: voltammetry, amperometry, biosensors, applications. Springer, (2015).
30. G. Ziyatdinova, and H. Budnikov. Electroanalysis of antioxidants in pharmaceutical dosage forms: state-of-the-art and perspectives. *Monatshefte Chem.-Chem. Monthly*, **146**: 741-753 (2015).
31. L.F. Mendes, A.R.S. de Silva, R.P. Bacil, S.H.P. Serrano, I. Angnes, T.R.L.C. Paixão, and W.R. de Araujo. Forensic electrochemistry: Electrochemical study and quantification of xylazine in pharmaceutical and urine samples. *Electrochimica Acta* **295**: 726-734 (2019).
32. D.A Mustafa, B.H. Mohammed, M.M. and Radhi. Oxidative and anti-oxidative effect of anesthesia compounds (ketamine and xylazine) on the rabbit blood sample using electrochemical method. *Rom. J. Neurol.* **19**: 76-83 (2020).
33. M.A. El-Shal, H.A.M. Hendawy. Highly sensitive voltammetric sensor using carbon nanotube and an ionic liquid composite electrode for xylazine hydrochloride, *Anal. Sci.* **35** (2):189–194 (2019).
34. K. Saisahas, A. Soleh, K. Promsuwan, A. Phonchai, N.S.M. Sadiq, W.K. Teoh, K.H. Chang, A.F.L. Abdullah, and W. Limbut. A portable electrochemical sensor for detection of the veterinary drug xylazine in beverage samples. *J. Pharm. Biomed. Anal.* **198**, p.113958 (2021).
35. K. Saisahas, A. Soleh, K. Promsuwan, J. Saichanapan, A. Phonchai, Sadiq, W.K. Teoh, K.H. Chang, A.F.L. Abdullah, and W. Limbut. Nanocoral-like polyaniline-modified graphene-based electrochemical paper-based analytical device for a portable electrochemical sensor for xylazine detection. *ACS omega*, **7**(16): 13913-13924 (2022).
36. L.F. de Lima, and W.R. de Araujo. Laser-scribed graphene on polyetherimide substrate: an electrochemical sensor platform for forensic determination of xylazine in urine and beverage samples. *Microchimica Acta*, **189** (12): 465 (2022).
37. S. Tajik, H. Beitollahi, F.G. Nejad, M. Safaei, K. Zhang, Q. Van Le, R.S. Varma, H.W. Jang, and M. Shokouhimehr. Developments and applications of nanomaterial-based carbon paste electrodes. *RSC advances* **10**: 21561-21581 (2020).
38. L. Qian, S. Durairaj, S. Prins, S. and A. Chen. Nanomaterial-based electrochemical sensors and biosensors for the detection of pharmaceutical compounds. *Biosen. Bioelectron.*, vol. **175**:112836 (2021).
39. A.S. Agnihotri, A. Varghese, and M. Nidhin. Transition metal oxides in electrochemical and bio sensing: A state-of-art review. *Applied Surface Sci. Adv.* **4**,100072 (2021).
40. I. Svancara, K. Kalcher, A. Walcarius, and K. Vytras. Electroanalysis with carbon paste electrodes. *Crc Press* (2019).
41. D. Stanković, E. Mehmeti, L. Svorc, and K. Kalcher. New electrochemical method for the determination of β -carboline alkaloids, harmalol and harmine, in human urine samples and in *Banisteriopsis caapi*. *Microchem. J.* **118**: 95-100 (2015).
42. Z. Zhang, and E. Wang. Electrochemical principles and methods, Science Press, Beijing, (2000).
43. V. Jouikov, and J. Simonet. Electrochemical reactions of sulfur organic compounds. *Encyclopedia of Electrochemistry: Online* (2007).
44. G.A. Mersal. Electrochemical applications and computational studies on ephedrine drug. *J. Solid State Electrochem.* **16**(6): 2031-2039 (2012).

-
45. D.K. Gosser. Cyclic voltammetry, simulation and analysis of reaction mechanisms, Wiley VCH, New York (1993).
46. N. Elgrishi, K.J. Rountree, B.D. McCarthy, E.S. Rountree, T.T. Eisenhart, and J.L. Dempsey. A practical beginner's guide to cyclic voltammetry. *J. Chem. Educ.* **95**: 197-206 (2018).
47. E. Laviron. Theoretical study of a reversible reaction followed by a chemical reaction in thin layer linear potential sweep voltammetry. *J. Electroanal. Chem. Interfacial Electrochem.* **39**: 1 (1972).
48. L.A. Currie, L.A. International recommendations offered on analytical detection and quantification concepts and nomenclature. *Anal. Chimica Acta* **391**: 103-134 (1999).
49. S.M. Ghoreishi, M. Behpour, and M. Golestaneh. Simultaneous determination of sunset yellow and tartrazine in soft drinks using gold nanoparticles carbon paste electrode. *Food Chem.* **132**(1): 637-641 (2012).